frontiers | Frontiers in Plant Science

TYPE Original Research
PUBLISHED 02 September 2022
DOI 10.3389/fpls.2022.996498

OPEN ACCESS

EDITED BY
Rajesh Chandra Misra,
John Innes Centre,
United Kingdom

REVIEWED BY
Youzhi Li,
Hunan Agricultural University,
China
Margot Schulz,
University of Bonn,
Germany

*CORRESPONDENCE
Yulong Feng
fyl@syau.edu.cn
Tong An
m18602463916@163.com

SPECIALTY SECTION
This article was submitted to Plant Metabolism and Chemodiversity, a section of the journal Frontiers in Plant Science

RECEIVED 17 July 2022
ACCEPTED 22 August 2022
PUBLISHED 02 September 2022

CITATION
Liu Z, Zhang N, Ma X, Zhang T, Li X, Tian G, Feng Y and An T (2022) Sesquiterpenes from *Ambrosia artemisiifolia* and their allelopathy.
Front. Plant Sci. 13:996498.
doi: 10.3389/fpls.2022.996498

Sesquiterpenes from *Ambrosia artemisiifolia* and their allelopathy

Zhixiang Liu[1,2], Nan Zhang[2], Xiaoqing Ma[2], Tong Zhang[2], Xuan Li[2], Ge Tian[2], Yulong Feng[1,2]* and Tong An[1,2]*

[1]College of Plant Protection, Shenyang Agricultural University, Shenyang, China, [2]College of Biological Science and Technology, Shenyang Agricultural University, Shenyang, China

Ambrosia artemisiifolia, an invasive plant, has seriously harmed the agricultural production, native ecosystems and human health. Allelopathy is an important reason for the successful invasion of this alien plant. However, the chemical basis, action effects, action mechanism and release pathway of its allelopathy remain unclear. To address these problems, four sesquiterpenes (**1**–**4**), consisting of three new sesquiterpenes (**1**–**2**, **4**), were isolated from the whole plant of *A. artemisiifolia* using a variety of column chromatography techniques, and identified using HR-ESIMS, 1D-NMR, 2D-NMR, and ECD. All the compounds exhibited different levels of inhibitory effects on three native plants (*Setaria viridis*, *Digitaria sanguinalis*, *Chenopodium album*) and one model plant (*Arabidopsis thaliana*), especially compound **1**. In addition, the preliminary action mechanism of active compound 1 was revealed by FDA/PI staining assay. Furthermore, the allelopathic substances **1**–**3** were released into environment through the root secretion pathway by UPLC-MS/MS analyses.

KEYWORDS

allelopathy, *Ambrosia artemisiifolia*, invasive plant, isolate, sesquiterpenes

Introduction

In recent decades, with the acceleration of globalization and world trade, the spread of invasive plants has been increasing, causing a serious threat to agricultural production and the ecological environment (Bonnamour et al., 2021). It is urgent to reveal the invasive mechanism of alien plants, which is necessary for risk assessment of invasive plants and to develop effective prevention methods. In recent years, the novel weapons hypothesis (NWH) has become a hot topic of research for investigating the invasion mechanism of alien plants (Callaway and Ridenour, 2004). The hypothesis suggests that the successful invasion of alien plants is largely due to their release of allelopathic substances that are relatively novel to native plants (Bais, 2003). The allelopathic substances are released into the environment through appropriate pathways, such as root secretion and rainwater leaching, to negatively affect the growth of native plants, enabling alien plants to gain advantages and promote their expansion into dominant single populations (Thorpe et al., 2009). Therefore, fully understanding the allelopathic effects of invasive plants on native

plants may help reveal the invasion mechanism of alien plants while also clarifying the chemical relationship between invasive plants and native plants, and this may enable new approaches for the utilization of invasive plants.

Ambrosia artemisiifolia L. (Asteraceae), which originated from North America, is an invasive weed found all over the world. The invader can inhibit the growth of native plants, destroying the original ecosystem and reducing agricultural production (Sun and Roderick, 2019). Furthermore, its pollen can cause a series of allergic reactions and directly affect human health (Zhao et al., 2017). Field observations have shown that *A. artemisiifolia* often forms a dominant single population with few other plants around it. The reason is not only that *A. artemisiifolia* has strong growth characteristics, but also its successful allelopathic effects on native plants. Previous studies reported that various solvent extracts of *A. artemisiifolia* had significant inhibitory effects on the growth and seed germination of *Lactuca sativa*, *Lycopersicon esculentum*, *Zea mays*, and other plants (Lehoczky et al., 2011; Vidotto et al., 2013; Bonea et al., 2018). These studies also confirmed that allelopathy is a major reason for the successful invasion of *A. artemisiifolia.* However, most studies only consider the effects of crude extract of *A. artemisiifolia* on native plants, and the chemical basis, action effects, action mechanism and release pathway of its allelopathy remain unclear. Like most higher plants, *A. artemisiifolia* contains a large number of secondary metabolites. Among them, sesquiterpenoids are the main chemical components, including the eudesmane-type, germacrane-type, bisabolane-type and guaiane-type, which have complex and variable structural frameworks (Taglialatela-Scafati et al., 2012; Ding et al., 2015; An et al., 2019). Studies have shown that sesquiterpenoids play an important role in plant allelopathy, which can significantly inhibit plant growth. Similarly, sesquiterpenoids may also be the potential allelopathic substances for *A. artemisiifolia* (Bennett and Wallsgrove, 1994; Chadwick et al., 2013).

In this study, to clarify the chemical basis of allelopathy, we isolated and identified the secondary metabolites from the whole plant of *A. artemisiifolia*. And the allelopathic effects of isolated compounds on three native plants (*Setaria viridis*, *Digitaria sanguinalis*, *Chenopodium album*) and one model plant (*Arabidopsis thaliana*) were also examined. In addition, the preliminary action mechanism of active compound **1** was revealed by FDA/PI staining assay. Furthermore, the release pathway of allelopathic substances was analyzed by UPLC-MS/MS analyses.

Materials and methods

General

Column chromatography was carried out using silica gel (Qingdao Marine, China), MCI (Mitsubishi, Japan), and Sephadex LH-20 (GE Healthcare, Sweden). RP-HPLC isolation was performed using a 1,260 system (Agilent, United States) coupled with a 250 mm × 10 mm, 5 μm XDB-C_{18} column (YMC, Japan). UV spectra were determined using a 241 spectrophotometer (Perkin Elmer, United States). HR-ESIMS spectra were measured using a 6,545 Q-TOF spectrometer (Agilent, United States). NMR spectra were recorded using an AV-600 instrument (Bruker, Germany). GC analysis was performed using a 7890A system (Agilent, United States). ECD spectra were obtained using a MOS-450 detector (Bio-Logic, France). Cell viability analyses were performed using an A1 laser confocal microscope (Nikon, Japan). UPLC-MS/MS analyses were performed using a 6,545 LC/Q-TOF system (Agilent, United States) coupled with a 50 mm × 2.1 mm, 1.9 μm EC-C_{18} column (Agilent, United States).

Plant material

The whole plant of *A. artemisiifolia* was collected from Shenyang, Liaoning Province, China (123° 48′ E, 42° 05′ N) in August 2020 and identified by Professor Bo Qu (Shenyang Agricultural University). A voucher specimen (20200811) was kept in the herbarium of Shenyang Agricultural University.

Extraction and isolation

The air-dried and powdered *A. artemisiifolia* (50 kg) were extracted with 80% ethanol at room temperature (200 L × 3, 7 days each time). The concentrated ethanol extract (1,200 g) was partitioned continuously with petroleum ether (5 L × 3) and ethyl acetate (5 L × 3). The ethyl acetate fraction (230 g) was then subjected to silica gel column chromatography eluted with a gradient of dichloromethane:methanol (99:1, 98:2, 95:5, 90:10, 80:20, 70:30, *v*/*v*) to yield five subfractions (Fr. A–E). Fr. D (18 g) was subjected to MCI column chromatography eluted with a gradient of methanol:H_2O (10:90, 30:70, 50:50, 70:30, *v*/*v*) to yield five subfractions (Fr. D-1–5). Fr. D-2 (2.1 g) was subjected to Sephadex LH-20 column chromatography eluted with isocratic of acetone to yield eight subfractions (Fr. D-2-1–8). Fr. D-2-3 (130 mg) was isolated using RP-HPLC (210 nm, 5.0 ml/min) eluted with isocratic of methanol:H_2O (20:80, *v*/*v*) to yield compounds **1** (10.2 mg, t_R = 32.4 min), **2** (3.5 mg, t_R = 17.5 min) and **3** (4.6 mg, t_R = 57.9 min), respectively. Similarly, Fr. D-2-5 (64 mg) was isolated using RP-HPLC (210 nm, 5.0 ml/min) eluted with isocratic of methanol:H_2O (15:85, *v*/*v*) to yield compound **4** (6.1 mg, t_R = 78.1 min).

Compound **1**: light yellow powder; UV (methanol) λ_{max} (logε): 219 (0.54) nm; ECD (methanol) λ_{max} ($\Delta\varepsilon$) 209 (−60.57), 228 (−11.81), 246 (+8.90) nm; HR-ESIMS at *m/z* 303.1206 $[M+Na]^+$ (calcd for $C_{15}H_{20}O_5Na$, 303.1208); ^1H and ^{13}C NMR data, see Table 1.

Compound **2**: light yellow oil; UV (methanol) λ_{max} (logε): 214.05 (0.20) nm; ECD (methanol) λ_{max} ($\Delta\varepsilon$) 226 (−54.63) nm; HR-ESIMS at *m/z* 321.1311 $[M+Na]^+$ (calcd for $C_{15}H_{22}O_6Na$, 321.1314); ^1H and ^{13}C NMR data, see Table 1.

TABLE 1 ^{1}H (600MHz) and ^{13}C NMR (150MHz) spectroscopic data of compounds 1–4 in methanol-d_4.

Position	1		2		3		4	
	δ_C	δ_H	δ_C	δ_H	δ_C	δ_H	δ_C	δ_H
1	76.2	3.42 (1H, dd, 11.8, 4.4)	76.3	3.36 (1H, dd, 12.4, 4.0)	75.6	3.42 (1H, dd, 12.2, 3.9)	131.5	
2	41.1	2.12 (1H, m) 1.55(1H, q, 11.8)	36.5	1.89 (1H, m) 1.68 (1H, q, 12.4)	34.0	1.94 (1H, m) 1.73 (1H, q, 12.2)	30.4	1.40 (1H, m) 1.28 (1H, m)
3	70.5	3.97 (1H, dd, 11.8. 5.1)	76.4	3.48 (1H, dd, 12.4, 4.5)	78.2	4.72 (1H, dd, 12.2, 4.6)	207.2	
4	148.0		76.3		74.9		138.2	
5	53.9	1.72 (1H, d, 11.0)	57.7	1.33 (1H, d, 11.5)	57.6	1.45 (1H, d, 12.0)	165.2	
6	79.8	5.20 (1H, d, 11.0)	81.1	5.30 (1H, d, 11.5)	80.6	5.31 (1H, d, 12.0)	78.8	5.41 (1H, d, 11.1)
7	169.3		169.8		169.5		56.4	2.14 (1H, m)
8	23.1	3.05 (1H, m) 2.50 (1H, td, 14.1, 5.7)	23.3	3.30 (1H, m) 2.49 (1H, td, 14.2, 5.6)	23.2	3.04 (1H, m) 2.50 (1H, td, 14.0, 5.5)	74.1	4.15 (1H, m)
9	37.8	2.23 (1H, m) 1.28 (1H, m)	41.2	2.17 (1H, m) 1.24 (1H, m)	41.0	2.18 (1H, m) 1.27 (1H, m)	42.6	2.88 (1H, dd, 15.2, 3.1) 2.35 (1H, dd, 15.2, 3.1)
10	42.6		42.3		42.2		133.3	
11	123.7		123.6		123.9		42.5	2.75 (1H, m)
12	175.6		174.6		174.5		180.0	
13	54.0	4.28 (2H, s)	54.0	4.28 (2H, s)	54.0	4.29 (2H, s)	14.9	1.32 (3H, d, 7.0)
14	10.9	0.90 (3H, s)	13.5	1.07 (3H, s)	13.5	1.10 (3H, s)	9.6	1.96 (3H, s)
15	106.7	5.37 (1H, s) 5.10 (1H, s)	17.4	1.35 (3H, s)	18.1	1.44 (3H, s)	25.5	1.94 (3H, s)
1′					172.2			
2′					21.0	2.06 (3H, s)		

Compound **3**: light yellow oil; UV (methanol) λ_{max} (logε): 213 (0.32) nm; ECD (methanol) λ_{max} ($\Delta\varepsilon$) 226 (−5.92) nm; HR-ESIMS at *m/z* 363.1417 $[M+Na]^+$ (calcd for $C_{17}H_{24}O_7Na$, 363.1420); ^{1}H and ^{13}C NMR data, see Table 1.

Compound **4**: light yellow oil; UV (methanol) λ_{max} (logε): 306 (0.11) nm; ECD (methanol) λ_{max} ($\Delta\varepsilon$) 231 (+32.86), 310 (+8.16) nm; HR-ESIMS at *m/z* 263.1289 $[M+H]^+$ (calcd for $C_{15}H_{19}O_4$, 263.1283); ^{1}H and ^{13}C NMR data, see Table 1.

ECD calculations

The ECD calculations of compounds **1**–**4** were conducted using Gaussian 09 (Liu et al., 2021). Firstly, the conformational analyses were initially performed using the MMFF94 force field. Then, the obtained conformations were further optimized at the B3LYP/6-31G (d) level. Subsequently, the optimized conformations were calculated using a TDDFT method at the B3LYP/6–311 + G (2d, p) level (methanol). Finally, based on the Boltzmann weighting of each conformer, the calculated ECD curves were generated.

Allelopathic assay

The allelopathic assay was performed as a previously described method with some modifications (Li et al., 2019). Firstly, the tested compounds were dissolved with DMSO and added to different volumes of 1/2 MS medium, respectively, to obtain the medium containing 100, 50, and 25 μM compounds, and the blank control contained the same volume of DMSO. Then, the 2 ml of medium was removed into the each well of 6-well plates, respectively. Subsequently, the seeds of *S. viridis*, *D. sanguinali*, *C. album*, *A. thaliana* were sterilized with 0.1% $HgCl_2$ and washed with sterilized water at least three times, respectively. After the medium had cooled naturally to a solid state, 8 to 10 sterilized seeds were evenly placed in a row on the medium and cultured vertically in an illumination incubator (three replicates per compound). Finally, when the roots of the blank control grew to the bottom of 6-well plates, the lengths of roots were measured. Inhibitory rate (%) was calculated as $(L_C - L_T)/Lc \times 100\%$, where L_C and L_T were the average lengths of blank control and compound-treated roots, respectively. Logran, a common herbicide, was used as a positive control.

Statistical analyses

The data of allelopathic assay were expressed as means ± SD of three replicates. One-way ANOVA was used to compare data between groups when the data followed a normal distribution. Differences were considered to be statistically significant if $p < 0.05$.

Cell viability analyses

The cell viability analyses were performed as a previously described method with some modifications (Pan et al., 2001). After the allelopathic assay, the root tips of *A. thaliana* (0.5 cm) were stained with a mixture of 12.5 μg/ml FDA (fluorescein diacetate) and 5 μg/ml PI (propidium iodide) for 10 min. Then, the roots were washed with distilled water and placed on slides. Finally, the roots were observed using a laser confocal microscope (excitation at 480 nm and emission at 520 nm). Red and green fluorescence represented dead and living cells, respectively.

Collection of root secretion and rainwater leaching

The collection of root secretion and rainwater leaching was performed as a previously described method with some modifications (Wang et al., 2015). The rhizosphere soil of *A. artemisiifolia* (200 g) was randomly collected at 5–10 cm depths and carefully picked out the roots. The soil samples were crushed to pass through a sieve (30 mesh). The sieved soil was extracted ultrasonically with methanol (1 L) at room temperature for 30 min. The extraction were then filtered and concentrated *in vacuo* to obtain the root secretion samples. The aerial part of *A. artemisiifolia* (10 living bodies) was washed with distilled water (5 L) for 10 min. The rinses were then collected and concentrated *in vacuo* to obtain the rainwater leaching samples.

UPLC-MS/MS analyses

The identification and quantification of compounds **1**–**4** in the root secretion and rainwater leaching samples of *A. artemisiifolia* were performed by UPLC-MS/MS. The solution of root secretion and rainwater leaching were filtered through a millipore filter (0.22 μm) before UPLC-MS/MS analyses (flow rate of 0.4 ml/min; injection volume of 1 μl; column temperature of 30°C), respectively. The mobile phase consisted of water containing 0.1% formic acid (A) and methanol (B) was programmed as follows: 0–5 min, B 10%; 5–20 min, B from 10% to 50%. Positive ionization was performed using the following settings: gas temperature, 280°C; drying gas flow, 8 L/ min; nebulizer, 35 psi; sheath gas temperature, 320°C; sheath gas flow, 12 L/ min; fragmentor, 145 V; skimmer, 65 V; oct 1 RF Vpp, 750 V. The identification of compounds in the root secretion and rainwater leaching was determined by comparing the retention times, MS, MS/MS spectra with those of isolated compounds **1**–**4**. The quantification of compounds in the root secretion and rainwater leaching was performed using the same method described above, with the isolated compounds as external standards. The standard curves were plotted using six concentrations (100, 10, 1, 0.1, 0.01, 0.001 μg/ml) and the corresponding ion peak area. The regression equations of compounds **1**–**3** were $y = 22{,}758x - 8415.2$ ($R^2 = 0.9996$), $y = 17{,}790x + 7201.4$ ($R^2 = 0.9996$) and $y = 20{,}732x - 5553.5$ ($R^2 = 0.9997$), respectively.

Results and discussion

Compound **1** was obtained as a light yellow powder with $C_{15}H_{20}O_5$ (six degrees of unsaturation) according to HR-ESIMS data (*m/z* 303.1206 $[M + Na]^+$, calcd for $C_{15}H_{20}O_5Na$, 303.1208). Its 1D-NMR spectra (Table 1) showed one carbonyl group [δ_C 175.6 (C-12)], two double bond groups [δ_H 5.37 (1H, s, H-15), 5.10 (1H, s, H-15); δ_C 169.3 (C-7), 148.0 (C-4), 123.7 (C-11), 106.7 (C-15)], one primary alcohol group [δ_H 4.28 (2H, s, H-13); δ_C 54.0 (C-13)], two secondary alcohol groups [δ_H 3.97 (1H, dd, $J = 11.8$, 5.1 Hz, H-3), 3.42 (1H, dd, $J = 11.8$, 4.4 Hz, H-1); δ_C 76.2 (C-1), 70.5 (C-3)], and one methyl group [δ_H 0.90 (3H, s, H-14); δ_C 10.9 (C-14)], respectively.

In the HMBC spectrum (Figure 1), the key correlations of H-3/C-2, C-4; H-6/C-5; H-8/C-7, C-9; H-14/C-1, C-5, C-9, C-10; H-15/C-3, C-5 established a eudesmane-type sesquiterpene moiety (An et al., 2019). The key correlations of H-6/C-11, C-12; H-13/C-7, C-11, C-12 established a isosiphonodin moiety (Caloprisco et al., 2002). In addition, the key correlations of H-6/C-5; H-8/C-7 revealed that the isosiphonodin moiety was connected to the eudesmane-type sesquiterpene moiety through C-6 and C-7. In the NOESY spectrum (Figure 2), the key correlations of H-1/H-3, H-5; H-14/H-6 indicated that H-1, H-3, H-5 and H-6, H-14 were oriented on the opposite side. Furthermore, the calculated ECD curve of (1*R*, 3*S*, 5*S*, 6*R*, 10*R*)-**1b** matched well with the experimental result of **1** (Figure 3). Thus, the planar and stereoscopic structure of compound **1** was constructed and named Eudesmanol A (Figure 4).

Compound **2** was obtained as a light yellow oil with $C_{15}H_{22}O_6$ (five degrees of unsaturation) according to HR-ESIMS data (*m/z* 321.1311 $[M + Na]^+$, calcd for $C_{15}H_{22}O_6Na$, 321.1314). Comparison of its 1D NMR spectra with Eudesmanol A showed that they were very similar except for one additional methyl group [δ_H 1.35 (3H, s, H-15); δ_C 17.4 (C-15)], one additional tertiary alcohol group [δ_C 76.3 (C-4)], and one missing terminal double bond group. In the HMBC spectrum (Figure 1), the key correlations of H-15/C-4, C-5 revealed that the methyl and hydroxyl groups were connected to Eudesmanol A by C-4. In the NOESY spectrum (Figure 2), the key correlations of H-1/H-3, H-5; H-6/H-14, H-15 indicated that H-1, H-3, H-5 and H-6, H-14, H-15 were oriented on the opposite side. Furthermore, the calculated ECD curve of (1*R*, 3*S*, 4*S*, 5*S*, 6*R*,

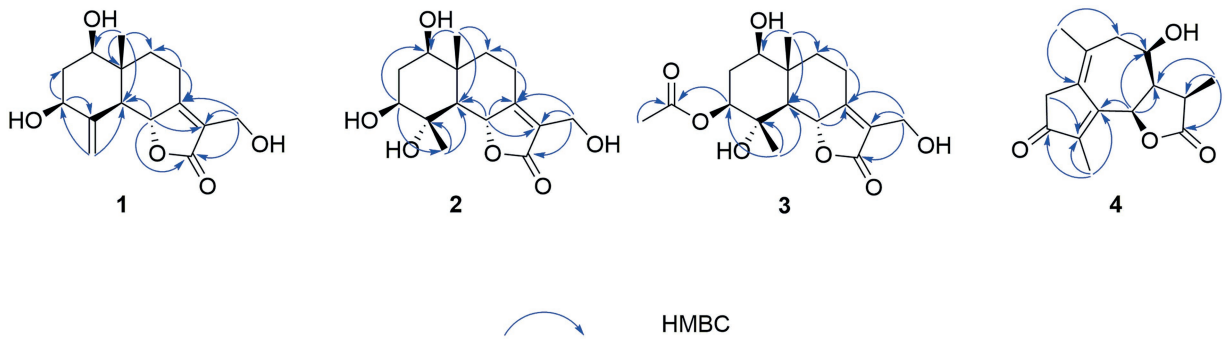

FIGURE 1
Key HMBC correlations of compounds **1–4**.

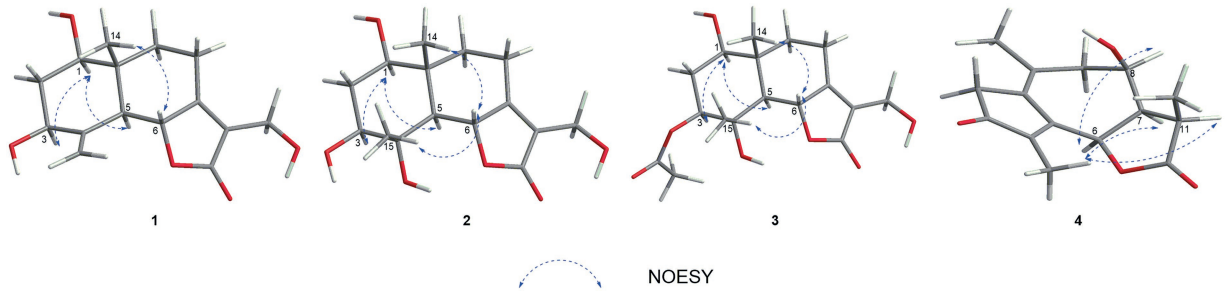

FIGURE 2
Key NOESY correlations of compounds **1–4**.

10*R*)-**2a** matched well with the experimental result of **2** (Figure 3). Thus, the planar and stereoscopic structure of compound **2** was constructed and named Eudesmanol B (Figure 4).

Compound **3** was obtained as a light yellow oil with $C_{17}H_{24}O_7$ (six degrees of unsaturation) according to HR-ESIMS data (*m/z* 363.1417 $[M+Na]^+$, calcd for $C_{17}H_{24}O_7Na$, 363.1420). Comparison of its 1D NMR spectra with a known compound 3*β*-Acetoxy-l*β*, 4*α*, 13-trihydroxyeudesm-7 (11)-*en*-6*α*, l2-olide showed that they were very similar except for the different deuterated solvents. In the HMBC spectrum (Figure 1), the key correlations revealed that compound **3** has the same planar structure as 3*β*-Acetoxy-l*β*, 4*α*, 13-trihydroxyeudesm-7 (11)-*en*-6*α*, l2-olide (Abdel-Mogi et al., 1989). In the NOESY spectrum (Figure 2), the key correlations of H-1/H-3, H-5; H-6/H-14, H-15 indicated that H-1, H-3, H-5 and H-6, H-14, H-15 were oriented on the opposite side. Furthermore, the calculated ECD curve of (1*R*, 3*S*, 4*S*, 5*S*, 6*R*, 10*R*)-**3a** matched well with the experimental result of **3** (Figure 3), which revealed that compound **3** has the same stereoscopic structure as 3*β*-Acetoxy-l*β*, 4*α*, 13-trihydroxyeudesm-7 (11)-*en*-6*α*, l2-olide. Thus, the planar and stereoscopic structure of compound **3** was constructed (Figure 4).

Compound **4** was obtained as a light yellow oil with $C_{15}H_{18}O_4$ (seven degrees of unsaturation) according to HR-ESIMS data (*m/z* 263.1289 $[M+H]^+$, calcd for $C_{15}H_{19}O_4$, 263.1283). Its 1D-NMR spectra (Table 1) showed two carbonyl groups [δ_C 207.2 (C-3), 180.0 (C-12)], two double bond groups [δ_C 165.2 (C-5), 138.2 (C-4), 133.3 (C-10), 131.5 (C-1)], one secondary alcohol group [δ_H 4.15 (1H, m, H-8); δ_C 74.1 (C-8)], three methyl groups [δ_H 1.96 (3H, s, H-14), 1.94 (3H, s), 1.32 (3H, d, J = 7.0 Hz); δ_C 25.5 (C-15), 14.9 (C-13), 9.6 (C-14)], respectively.

In the HMBC spectrum (Figure 1), the key correlations of H-2/C-4; H-6/C-5, C-7, C-8; H-9/C-8; H-14/C-3, C-4, C-5; H-15/C-1, C-9 established a guaiane-type sesquiterpene moiety (Ding et al., 2015). The key correlations of H-6/C-7; H-13/C-7, C-11, C-12 established a *α*-methylbutyzolactone moiety (Simonaitis and Pitts, 1969). In addition, the key correlations of H-6/C-5, C-7, C-8 revealed that the *α*-methylbutyzolactone moiety was connected to the guaiane-type sesquiterpene moiety by C-6 and C-7. In the NOESY spectrum (Figure 2), the key correlations of H-7/H-6; H-8/H-6; H-11/H-6 indicated that H-6, H-7, H-8, H-11 and H-13 were oriented on the opposite side. Furthermore, the calculated ECD curve of (6*R*, 7*R*, 8*R*, 11*R*)-**4a** matched well with the experimental result of **4** (Figure 3). Thus, the planar and stereoscopic structure of compound **4** was constructed and named Guaianin (Figure 4).

Moreover, we assessed the allelopathic effects of compounds **1**–**4** from *A. artemisiifolia* on the root elongation of *S. viridis*, *D. sanguinali*, *C. album*, *A. thaliana*. As shown in

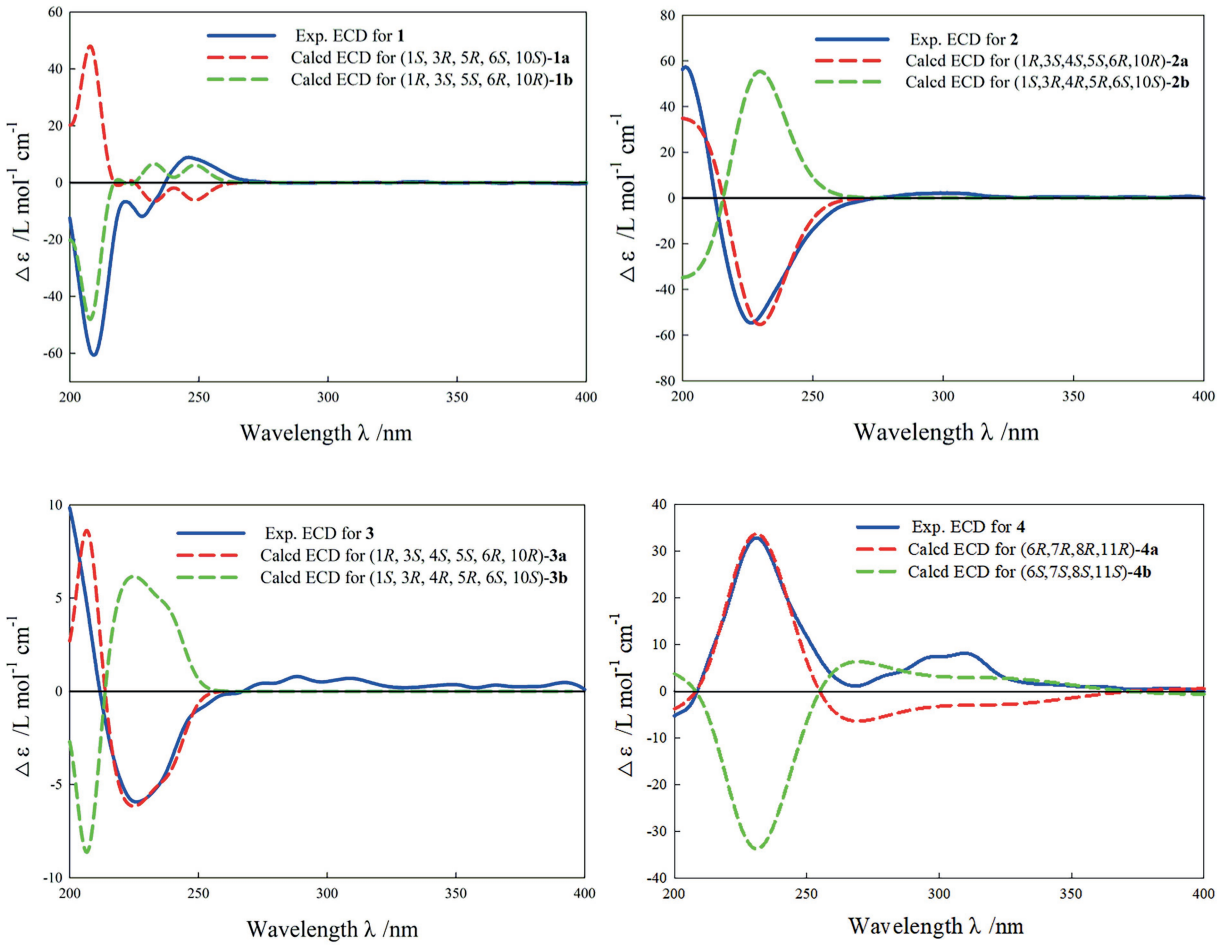

FIGURE 3
Experimental and calculated ECD curve of compounds **1–4**.

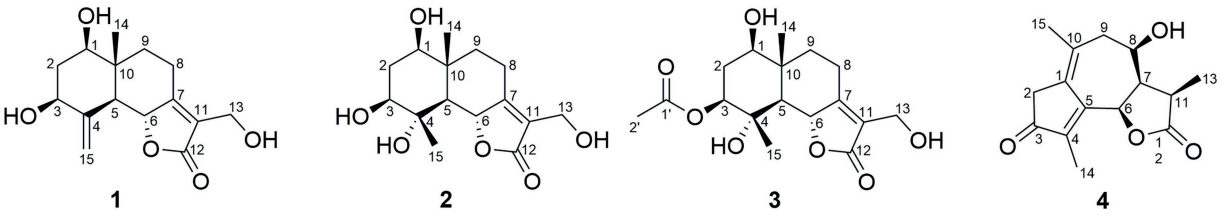

FIGURE 4
Structures of compounds **1–4**.

Figure 5, all of the compounds exhibited different levels of allelopathic effects. Compounds **1–3** exhibited moderate allelopathic effects with inhibition rates ranging from 15.60% to 73.42% at 100 μM. In addition, compound **4** exhibited slight allelopathic effects, and promoted the root elongation of three kinds of *S. viridis*, *D. sanguinali*, *A. thaliana* at low concentrations. Notably, compound **1** showed potent allelopathic effects (73.42% ± 8.54% on *S. viridis*, 51.23% ± 4.12% on *D. sanguinali*, 69.88% ± 8.09% on *C. album*, 59.34% ± 5.80% on *A. thaliana*, respectively) with more than 50% inhibitory rate at 100 μM, which approached the results observed for Logran. Comparisons of the structure–activity relationships of compounds **1–3** showed that the eudesmane-type sesquiterpenes with a terminal double bond group at C-4 may have greater allelopathic effects than the compounds with hydroxyl and methyl groups at C-4.

When plants are subjected to external stress, the cell viability changes. Thus, cell viability can be used as an important indicator for evaluating the allelopathic effects of compounds on plants (Yan et al., 2016). The preliminary action mechanism of active compound **1** was revealed by FDA/PI staining assay. As shown in Figure 6, the root tips of *A. thaliana* began to show red fluorescence at 25 μM of compound **1**, indicating that compound **1** could cause the partial cell death of *A. thaliana* at a low concentration. Additionally, when the concentration of compound **1** was 100 μM, the red fluorescence was dominant and green fluorescence was reduced in the root tips of *A. thaliana*. The results showed that the cell viability of root tips of *A. thaliana* decreased with increasing concentrations of compound **1**. Therefore, we speculated that compound **1** could play an allelopathic role by decreasing the cell viability of plants. However, the reason why the plant cell viability was decreased by compound **1** needs to be explored further.

It is well-known that allelopathic substances can play their allelopathic roles only when they are released into environment through appropriate pathways (Thorpe et al., 2009). To determine the allelopathic release pathway of the sesquiterpenes **1**–**4**, UPLC-MS/MS analyses were carried out to detect root secretion and rainwater leaching of *A. artemisiifolia*. According to their TIC chromatogram (Figure 7), compounds **1**–**3** had retention times of 4.42, 1.67, and 8.29 min, respectively, and they were detected in the root secretion of *A. artemisiifolia*., but no compounds were detected in rainwater leaching. The concentrations of compounds **1**–**3** in the rhizosphere soil were also determined as 0.55 ± 0.06, 0.44 ± 0.03, 0.48 ± 0.04 μg/g, respectively. The results indicated that

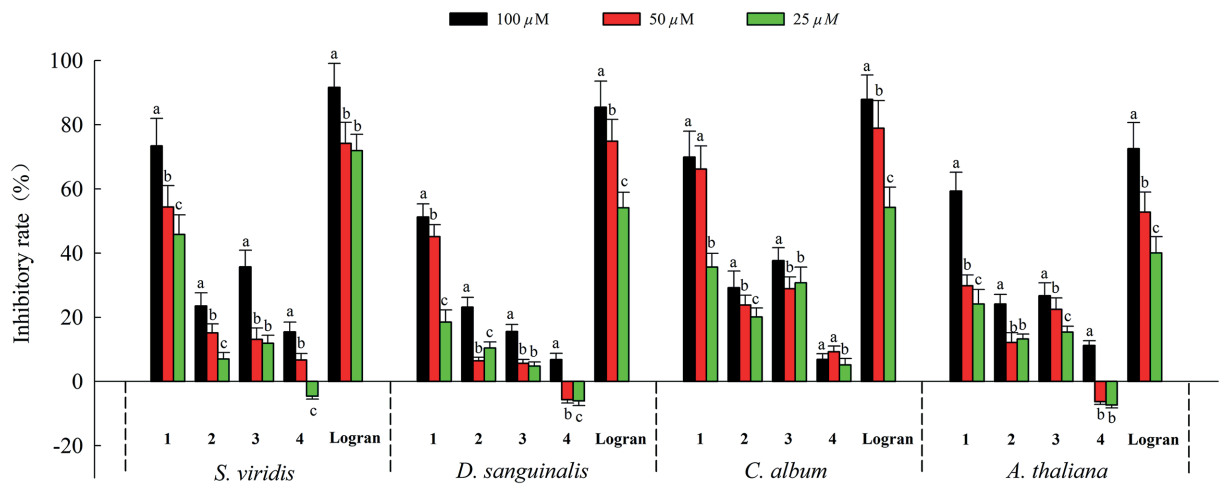

FIGURE 5
Allelopathic effects of compounds **1**–**4** on root growth of weeds. Different letters indicate significant differences between concentration treatments (p<0.05).

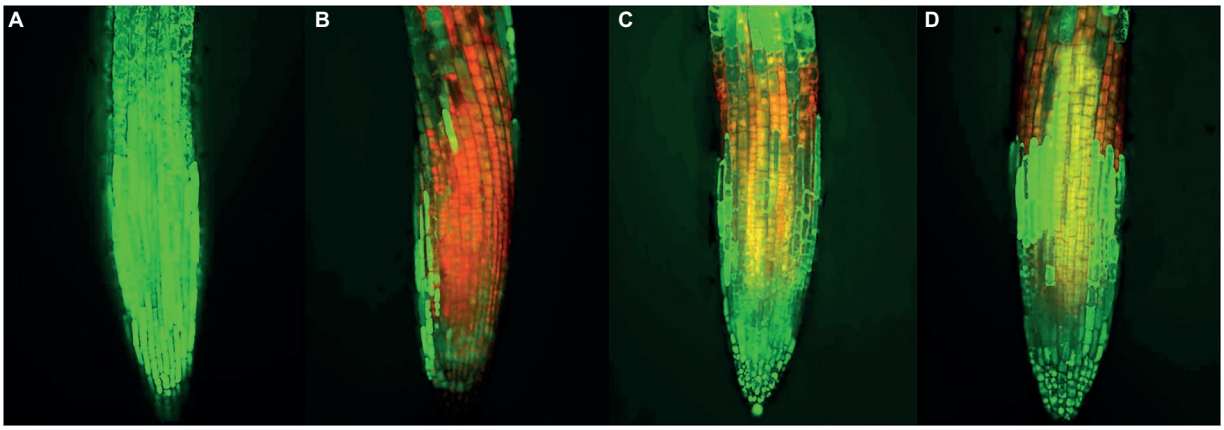

FIGURE 6
Effects of compound **1** on cell viability of the root tips of *Arabidopsis thaliana*. at concentrations of **(A)** 0, **(B)** 100, **(C)** 50, and **(D)** 25μM, respectively. Red and green fluorescence represented dead and living cells, respectively.

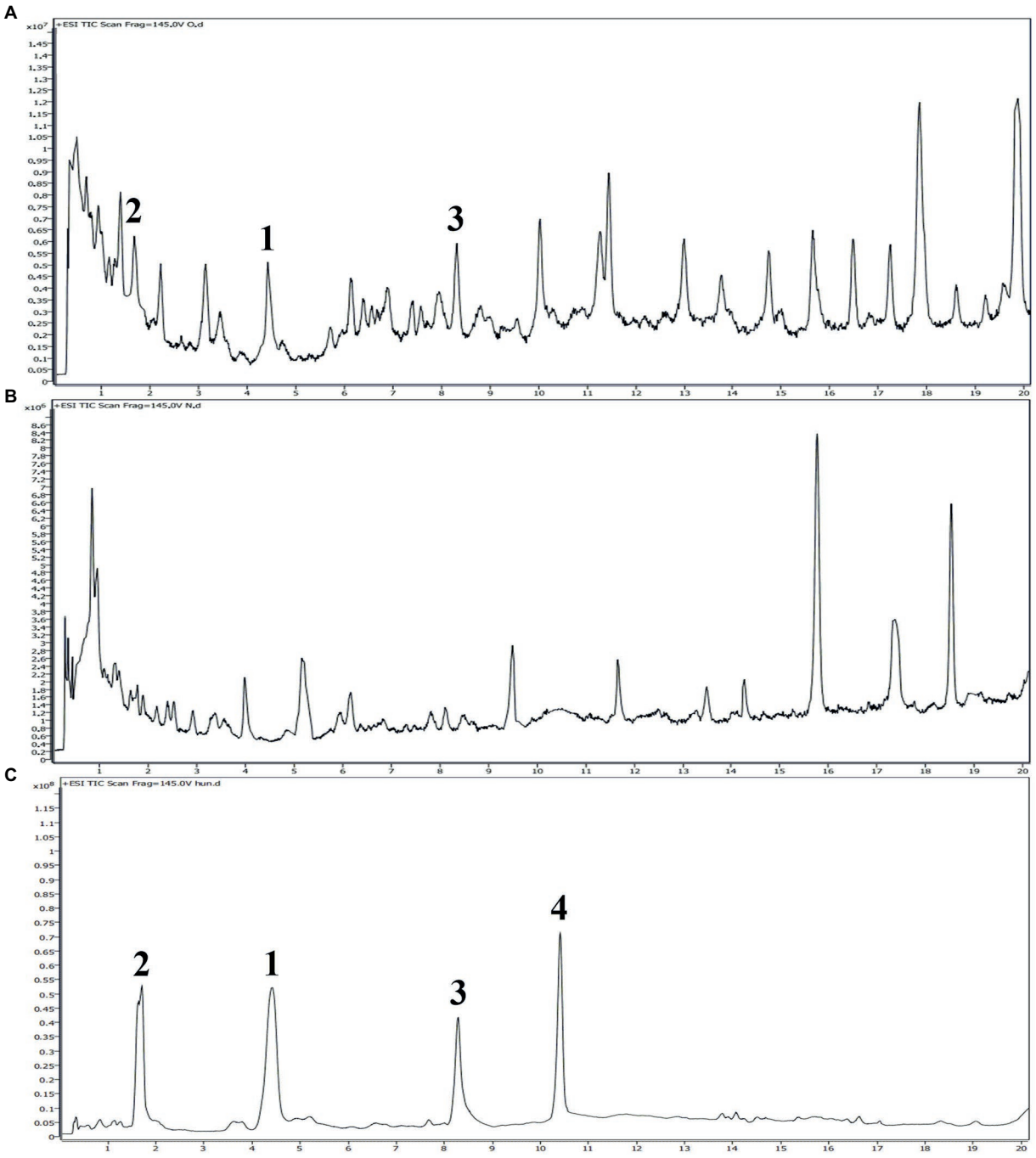

FIGURE 7
UPLC-MS/MS analyses of the root secretion, rainwater leaching, and isolated compounds from *Ambrosia artemisiifolia*. **(A)** TIC chromatogram of the root secretion from *A. artemisiifolia*; **(B)** TIC chromatogram of the rainwater leaching from *A. artemisiifolia*; **(C)** TIC chromatogram of compounds **1**–**4** from *A. artemisiifolia*.

the active compounds **1**–**3** were released into environment through root secretion to negatively affect the growth of native plants. Since the content of compounds **1**–**3** in the rhizosphere soil is low, we speculated that *A. artemisiifolia* could accumulate these compounds to achieve effective inhibitory concentrations only under certain conditions (e.g., when competing with other weeds; Kong et al., 2018). However, their dynamic release process remains unclear in the actual environment. Compound **4** was not detected in root secretion, possibly because of its rapid degradation by soil microorganisms or low water solubility. In addition, the lack of compounds in the rainwater leaching may be caused by the short washing times with distilled water, the replacement of distilled

water for rainwater, or the absence of compounds **1**–**4** in the aerial part of *A. artemisiifolia*.

In recent years, invasive plants have brought serious ecological, economic and social problems around the world. To effectively control these alien plants, it is of great theoretical and practical significance to clarify their invasion mechanisms (Enders et al., 2020). Numerous studies have shown that allelopathy is a driving factor in the successful invasion of alien plants (Yuan et al., 2021). For example, alien plants can release allelopathic substances that are relatively novel to native plants, thus negatively affecting on the growth of native plants. Sesquiterpenoids are abundant in many invasive plants, which play an important role in plant allelopathy and can significantly inhibit plant growth (Bennett and Wallsgrove, 1994; Chadwick et al., 2013) In our study, three eudesmane-type sesquiterpenes (**1**–**3**) with potent allelopathic effects were isolated and identified from *A. artemisiifolia*. These active compounds can be released into environment through the root secretion pathway to affect the cell viability of surrounding plants, thus promoting the invasion of *A. artemisiifolia*. We speculated that native plants have not yet adapted to these compounds (**1**–**3**) because of their novel structures and the lack of coevolution between alien and native plants. However, further research is needed to determine whether these compounds are already present in the original areas of invasive plants and how they specifically affect local plants. In addition, sesquiterpenoids generally have strong phytotoxic activities against many weeds (Anese et al., 2015; Masi et al., 2020). Moreover, allelopathic substances have the advantages of safety, easy degradation and no resistance to weed control (Macías et al., 2019). Therefore, the allelopathic sesquiterpenes (**1**–**3**) from *A. artemisiifolia* can be used to develop novel botanical herbicides and reduce the use of synthetic herbicides.

Conclusion

In summary, four sesquiterpenes (**1**–**4**), consisting of three eudesmane-type sesquiterpenes, one guaiane-type sesquiterpene, were isolated from the whole plant of *A. artemisiifolia* by a variety of column chromatography techniques. Their planar and stereoscopic structures were identified using HR-ESIMS, 1D-NMR, 2D-NMR, and ECD. All the compounds exhibited different levels of allelopathic effects on three native plants (*S. viridis*, *D. sanguinalis*, *C. album*) and one model plant (*A. thaliana*), but in particular, compound **1** significantly inhibited the root elongation of plants at 100 μM. In addition, active compound **1** decreased cell viability by exerting allelopathic effects, as observed by FDA/PI staining assay. Furthermore, the eudesmane-type sesquiterpenes (**1**–**3**) were mainly released into environment through the root secretion pathway, which was revealed by UPLC-MS/MS analyses. Our findings not only helped to reveal the invasion mechanism of *A. artemisiifolia* from the perspective of allelopathy, but also supported a promising strategy for its exploitation in herbicides.

Data availability statement

The original contributions presented in the study are included in the article/Supplementary material, further inquiries can be directed to the corresponding authors.

Author contributions

ZL designed the research, performed the experiments, analyzed the data, and wrote the manuscript. NZ, XM, TZ, XL, and GT performed the experiments and analyzed the data. YF and TA reviewed and revised the draft. All authors contributed to the article and approved the submitted version.

Funding

This research was supported by the National Natural Science Foundation of China (31700472).

Acknowledgments

We wish to thank Shihong Luo, Juan Hua, and Mingchao Liu from Shenyang Agricultural University for their assistance in allelopathic assay and UPLC-MS/MS analyses.

Conflict of interest

The authors declare that the research was conducted in the absence of any commercial or financial relationships that could be construed as a potential conflict of interest.

Publisher's note

Supplementary material

The Supplementary material for this article can be found online at: https://www.frontiersin.org/articles/10.3389/fpls.2022.996498/full#supplementary-material

References

Abdel-Mogi, M., Jakupovi, J., Dawidar, A. M., Metwallyb, M. A., and Abou-Elzahabb, M. (1989). Glaucolides from *Achillea fragrantissima*. *Phytochemistry* 28, 3528–3530. doi: 10.1016/0031-9422(89)80381-4

An, J. P., Ha, T. K. Q., Kim, H. W., Ryu, B., Kim, J., Park, J., et al. (2019). Eudesmane glycosides from *Ambrosia artemisiifolia* (common ragweed) as potential neuroprotective agents. *J. Nat. Prod.* 82, 1128–1138. doi: 10.1021/acs.jnatprod.8b00841

Anese, S., Jatobá, L. J., Grisi, P. U., Gualtieri, S. C. J., Santos, M. F. C., and Berlinck, R. G. S. (2015). Bioherbicidal activity of drimane sesquiterpenes from *Drimys brasiliensis* Miers roots. *Ind. Crop Prod.* 74, 28–35. doi: 10.1016/j.indcrop.2015.04.042

Bais, H. P. (2003). Allelopathy and exotic plant invasion: from molecules and genes to species interactions. *Science* 301, 1377–1380. doi: 10.1126/science.1083245

Bennett, R. N., and Wallsgrove, R. M. (1994). Secondary metabolites in plant defence mechanisms. *New Phytol.* 127, 617–633. doi: 10.1111/j.1469-8137.1994.tb02968.x

Bonea, D., Bonciu, E., Niculescu, M., and Olaru, A. L. (2018). The allelopathic, cytotoxic and genotoxic effect of *Ambrosia artemisiifolia* on the germination and root meristems of *Zea mays*. *Caryologia* 71, 24–28. doi: 10.1080/00087114.2017.1400263

Bonnamour, A., Gippet, J. M. W., Bertelsmeier, C., and Gurevitch, J. (2021). Insect and plant invasions follow two waves of globalisation. *Ecol. Lett.* 24, 2418–2426. doi: 10.1111/ele.13863

Callaway, R. M., and Ridenour, W. M. (2004). Novel weapons: invasive success and the evolution of increased competitive ability. *Front. Ecol. Environ.* 2, 436–443. doi: 10.1890/1540-9295(2004)002[0436:nwisat]2.0.co;2

Caloprisco, E., Fourneron, J. D., Faure, R., and Demarne, F. E. (2002). Unusual lactones from *Cananga odorata* (Annonaceae). *J. Agric. Food Chem.* 50, 78–80. doi: 10.1021/jf0105079

Chadwick, M., Trewin, H., Gawthrop, F., and Wagstaff, C. (2013). Sesquiterpenoids lactones: benefits to plants and people. *Int. J. Mol. Sci.* 14, 12780–12805. doi: 10.3390/ijms140612780

Ding, W. B., Huang, R., Zhou, Z. S., and Li, Y. Z. (2015). New sesquiterpenoids from *Ambrosia artemisiifolia* L. *Molecules* 20, 4450–4459. doi: 10.3390/molecules20034450

Enders, M., Havemann, F., Ruland, F., Bernard-Verdier, M., Catford, J. A., Gómez-Aparicio, L., et al. (2020). A conceptual map of invasion biology: integrating hypotheses into a consensus network. *Glob. Ecol. Biogeogr.* 29, 978–991. doi: 10.1111/geb.13082

Kong, C. H., Zhang, S. Z., Li, Y. H., Xia, Z. C., Yang, X. F., Meiners, S. J., et al. (2018). Plant neighbor detection and allelochemical response are driven by root-secreted signaling chemicals. *Nat. Commun.* 9:3867. doi: 10.1038/s41467-018-06429-1

Lehoczky, E., Glya, G., Szab, R., and Szalai, A. (2011). Allelopathic effects of ragweed (*Ambrosia artemisiifolia* L.) on cultivated plants. *Commun. Agric. Appl. Biol. Sci.* 76, 545–549.

Li, Y. L., Zhu, R. X., Li, G., Wang, N. N., Liu, C. Y., Zhao, Z. T., et al. (2019). Secondary metabolites from the endolichenic fungus *Ophiosphaerella korrae*. *RSC Adv.* 9, 4140–4149. doi: 10.1039/c8ra10329a

Liu, Z. X., Wang, M. Q., Tian, M. X., Yuan, L. L., Yu, B. M., Qu, B., et al. (2021). Pyrrole alkaloids from *Solanum rostratum* and their chemical defense function against *Henosepilachna vigintioctomaculata*. *Fitoterapia* 155:105031. doi: 10.1016/j.fitote.2021.105031

Macías, F. A., Mejías, F. J. R., and Molinillo, J. M. G. (2019). Recent advances in allelopathy for weed control: from knowledge to applications. *Pest Manag. Sci.* 75, 2413–2436. doi: 10.1002/ps.5355

Masi, M., Pannacci, E., Santoro, E., Zermane, N., Superchi, S., and Evidente, A. (2020). Stoechanones A and B, phytotoxic copaane sesquiterpenoids isolated from *Lavandula stoechas* with potential herbicidal activity against *Amaranthus retroflexus*. *J. Nat. Prod.* 83, 1658–1665. doi: 10.1021/acs.jnatprod.0c00182

Pan, J. W., Zhu, M. Y., and Chen, H. (2001). Aluminum-induced cell death in root-tip cells of barley. *Environ. Exp. Bot.* 46, 71–79. doi: 10.1016/s0098-8472(01)00083-1

Simonaitis, R., and Pitts, J. N. (1969). Molecular structure and photochemical reactivity. XI. Wavelength and methyl substituent effects in the photochemistry of lactones in the liquid phase. *J. Am. Chem. Soc.* 91, 108–112. doi: 10.1021/ja01029a023

Sun, Y., and Roderick, G. K. (2019). Rapid evolution of invasive traits facilitates the invasion of common ragweed, *Ambrosia artemisiifolia*. *J. Ecol.* 107, 2673–2687. doi: 10.1111/1365-2745.13198

Taglialatela-Scafati, O., Pollastro, F., Minassi, A., Chianese, G., Petrocellis, L. D., Marzo, V. D., et al. (2012). Sesquiterpenoids from common ragweed (*Ambrosia artemisiifolia* L.), an invasive biological polluter. *Eur. J. Org. Chem.* 2012, 5162–5170. doi: 10.1002/ejoc.201200650

Thorpe, A. S., Thelen, G. C., Diaconu, A., and Callaway, R. M. (2009). Root exudate is allelopathic in invaded community but not in native community: field evidence for the novel weapons hypothesis. *J. Ecol.* 97, 641–645. doi: 10.1111/J.1365-2745.2009.01520.X

Vidotto, F., Tesio, F., and Ferrero, A. (2013). Allelopathic effects of *Ambrosia artemisiifolia* L. in the invasive process. *Crop Prot.* 54, 161–167. doi: 10.1016/j.cropro.2013.08.009

Wang, Y., Luo, S. H., Hua, J., Liu, Y., Jing, S. X., Li, X. N., et al. (2015). Capitate glandular trichomes of *Paragutzlaffia henryi* harbor new phytotoxic labdane diterpenoids. *J. Agric. Food Chem.* 63, 10004–10012. doi: 10.1021/acs.jafc.5b04113

Yan, Z. Q., Wang, D. D., Cui, H. Y., Zhang, D. H., Sun, Y. H., Jin, H., et al. (2016). Phytotoxicity mechanisms of two coumarin allelochemicals from *Stellera chamaejasme* in lettuce seedlings. *Acta Physiol. Plant.* 38:248. doi: 10.1007/s11738-016-2270-z

Yuan, L., Li, J. M., Yu, F. H., Oduor, A. M. O., and Kleunen, M. V. (2021). Allelopathic and competitive interactions between native and alien plants. *Biol. Invasions* 23, 3077–3090. doi: 10.1007/s10530-021-02565-w

Zhao, F., Durner, J., Winkler, J. B., Traidl-Hoffmann, C., Strom, T. M., Ernst, D., et al. (2017). Pollen of common ragweed (*Ambrosia artemisiifolia* L.): Illumina-based de novo sequencing and differential transcript expression upon elevated NO_2/O_3. *Environ. Pollut.* 224, 503–514. doi: 10.1016/j.envpol.2017.02.032